Journal of Mines, Metals and Fuels, *71(12B) : 269-276; 2023. DOI: 10.18311/jmmf/2023/45622*

Print ISSN : 0022-2755

Journal of Mines, Metals and Fuels

Contents available at: *www.informaticsjournals.com/index.php/jmmf*

From Powders to Alloys: A Study of the Mechanical Alloying Process and Sintering

Rayappa Shrinivas Mahale[1,2*], Shamanth Vasanth[1], P. C. Sharath[3], R. Shashanka[4], Gangadhar M. Kanaginahal[2], Vaibhav Raibole[2], Krishnamurthy Goggi[2], Adarsh Patil[5] and S. B. Angadi[6]

[1]School of Mechanical Engineering, REVA University, Bengaluru - 560064, Karnataka, India; rayappamahale@gmail.com

[2]Department of Mechanical Engineering, Jain College of Engineering and Research, Udyambag, Belagavi - 590008, Karnataka, India

[3]Department of Electronics and Communication, Faculty of Engineering and Technology, Jain Deemed to be University, Bengaluru - 562112, Karnataka, India

[4]Department of Metallurgical and Materials Engineering, BARTIN University, Bartin - 74100, Turkey

[5]School of Mechanical Engineering, KLE Technological University, Hubballi - 580031, Karnataka, India

[6]Department of Mechanical Engineering, KLE Dr. M. S. Sheshgiri College of Engineering and Technology, Belagavi - 90008, Karnataka, India

Abstract

This study explores the intricacies of mechanical alloying, aiming to unlock its potential in modern engineering. It investigates the impact of milling duration, ball-to-powder ratio, and sintering temperature on the microstructure and mechanical properties of Al-7Zn-2.5Mg-2.5Cu alloy and Al7075 alloy. Mechanical alloying can produce alloys with exceptional hardness, strength, and ductility, while grain size can be controlled by adjusting milling parameters. Experimental techniques like X-Ray diffraction and transmission electron microscopy reveal microstructural changes during mechanical alloying, aiding in understanding metastable phases and element segregation, which influence the alloy's properties. Sintering, the subsequent consolidation step, determines final properties, with a trade-off between grain size and mechanical qualities observed at different sintering temperatures. This trade-off presents an intriguing avenue for developing materials with optimal properties. The study also explores potential applications of mechanical alloying across industries, including aerospace, biomedical, and energy. These unique mechanical alloys are attractive for various uses, from structural to catalytic and magnetic materials. They have the potential to revolutionize industries and drive technological advancements.

Keywords: *Ball to Powder Ratio, Mechanical Alloying, Mechanical Properties, Milling Duration, Sintering*

1.0 Introduction

1.1 Background

The demand for advanced alloys, exemplified by the Al-Zn-Mg-Cu alloy system, has surged due to their exceptional blend of strength, corrosion resistance, and low density, making them ideal for aerospace, automotive, and structural engineering applications. However, refining the microstructures and optimizing mechanical properties pose challenges, particularly in preventing coarse precipitates that can weaken ductility[1-5]. Innovative techniques like High-Pressure Torsion (HPT) and pre-stretching have been harnessed

**Author for correspondence*

to enhance Al-Zn-Mg-Cu alloy microstructures, resulting in smaller and more evenly distributed precipitates. These processes bolster mechanical properties by ensuring nanocrystalline structures with heightened strength, hardness, and resistance to wear and corrosion. Alongside this alloy system, Al7075 alloy has received significant attention for its remarkable tensile strength and utility in aerospace, automotive, and military sectors. It achieves its strength through finely dispersed Guinier-Preston zones and η_0 phase, with grain size refinement augmenting its robustness. While conventional methods limit grain size, techniques like Equal Channel Angular Pressing (ECAP) create sub-micrometre grain sizes. Yet, maintaining microstructural stability at elevated temperatures remains a challenge, with observed grain growth after annealing.

Mechanical alloying enhances grain refinement, primary phase dissolution, and fine secondary phase precipitation, boosting material strength. Powder metallurgy processes typically require high temperatures and extended sintering, potentially causing coarsening of strengthening particles and grain growth. Spark Plasma Sintering (SPS) and Field-Assisted Sintering Technology (FAST) mitigate these issues by using pressure and pulsed DC heating to maintain microstructure. Disrupting oxide layers at contact points reduces porosity. Numerous studies explore powder metallurgy methods for Al7075 alloy, yielding varied outcomes in terms of microstructural preservation and porosity control[6-11]. The incorporation of Zr as an alloying element shows promise in producing sub-microcrystalline microstructures with minimal porosity. Understanding these processes and their effects on thermal stability can lead to advanced materials for demanding engineering applications. Combining mechanical alloying and spark plasma sintering holds potential for future multi-component nanocrystalline bulk aluminium alloys. This research encompasses both the Al-Zn-Mg-Cu alloy system and Al7075 alloy as case studies, contributing to the understanding of nanocrystalline approaches and their influence on alloy properties. Insights gained will guide the optimization of mechanical alloying and sintering techniques for advanced alloys, critical for industries requiring high-performance materials such as aerospace and transportation. Case Study 1 delves into the Al-Zn-Mg-Cu alloy, examining experimental results, microstructural analysis, and mechanical properties. Case Study 2 investigates the Al7075 alloy, emphasizing its unique characteristics and the impact of milling and sintering processes on microstructure and properties. These case studies offer a comprehensive understanding of mechanical alloying and sintering techniques for advanced alloy fabrication[12-16].

2.0 Experimental Procedure, Material Preparation and Selection

High-purity elemental powders of aluminium (Al), zinc (Zn), magnesium (Mg), and copper (Cu) were used to create the Al-7Zn-2.5Mg-2.5Cu alloy. Rigorous measures ensured purity and homogeneity, with Al at 99.5% purity and mesh sizes of 38-75 **μm**, Zn, and Cu at 99.99% purity with mesh sizes of 4-23 **μm** for Zn and 3-20 **μm** for Cu, and Mg at 99% purity with mesh sizes of 75-150 **μm**. Cheng et al. employed a systematic procedure, drying the powders in a vacuum oven, combining them in a stainless-steel vacuum tank, and mechanically alloying them in a planetary ball mill under argon atmosphere. A ball-to-powder mass ratio of 20:1 was used with stainless-steel balls, and milling occurred at 400 RPM with intermittent pauses. Milling durations ranged from 5 to 40 hours, followed by vacuum drying and sintering in a graphite mold under controlled conditions[18-20]. Gradual cooling in a vacuum chamber ensured proper solidification,

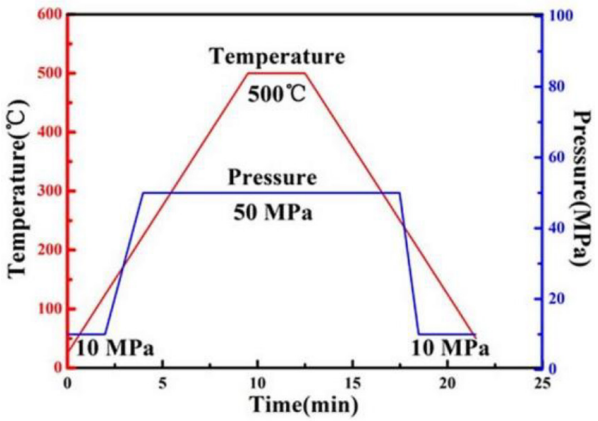


Figure 1: Temperature and pressure variations during sintering[17].

and samples were labelled based on milling times (P5 to P40) and corresponding sintered samples (S5 to S40) for subsequent analysis. Al7075, an age-hardenable aluminium alloy, was studied to improve its mechanical properties via mechanical milling. Gas-atomized powder underwent sieving, mechanical milling, and sintering to achieve an average particle size of 22.6 µm. Sintering involved 5 MPa pressure, temperature ramping at 80 degrees Celsius per minute, a 2-minute hold, and pressure release. High-temperature stability was evaluated after annealing at 425^{0}C for 1 hour, followed by rapid quenching in water. Characterization techniques included Light Microscopy (LM), Scanning Electron Microscopy (SEM), and Energy-Dispersive X-ray Spectroscopy (EDS), revealing irregular particle shapes and varied phases with zinc being the most abundant element. Transmission/Scanning Transmission Electron Microscopy (TEM/STEM) provided high-resolution microstructure images, while Focused Ion Beam (FIB) milling prepared TEM foils. Microhardness measurements assessed hardness, and X-Ray Diffraction (XRD) identified phases in the powder and compacts. The results suggest that Spark Plasma Sintering (SPS) can produce high-strength, high-toughness aluminium alloy components with fine microstructures and high hardness, though further parameter optimization is required[21-25].

3.0 Case Study 1: Analysis Al-7Zn-2.5Mg-2.5Cu Alloy

The morphological evolution of Al-7Zn-2.5Cu-2.5Mg milled powders followed distinct stages during ball milling: flattening, welding, fracture, formation of equiaxed particles, and dynamic equilibrium. Equiaxed particles emerged after 20 hours of milling, reaching a stable size distribution by 30 hours, with a slight size increase at 40 hours, signifying dynamic equilibrium. Increased milling time intensified plastic deformation, strain accumulation, and work hardening, leading to progressive particle fracture and size reduction. The cross-sectional analysis revealed lamellar internal morphology at 10 hours, transitioning to equiaxed particles with reduced internal pores at 30 hours, indicating enhanced internal densification due to grinding ball pressure, thereby improving properties like strength and ductility. XRD patterns showed no new phases but broadening and decreasing intensities of diffraction peaks for Al, Zn, Mg, and Cu as milling time increased. After 30 hours, diffraction peaks of Zn, Mg, and Cu disappeared, indicating their dissolution into the Al matrix. Intensive collisions and inter-diffusion of alloying elements led to a supersaturated solid solution, enhancing properties. Localized XRD patterns displayed peak broadening and shift towards larger angles, attributed to the incorporation of smaller atomic radius Zn, Cu, and Mg atoms, causing lattice distortion, increased yield strength, and hardness. Williamson-Hall analysis revealed gradual reduction in the average grain size of Al alloy powders with milling time, stabilizing after 30 hours, suggesting effective microstructure refinement through ball milling[28].

$$\beta \cos \theta = 0.9\lambda/d + 4\varepsilon \sin \theta \text{ ----------(1)}$$

The mechanical alloying process significantly influenced the microstructure and properties of

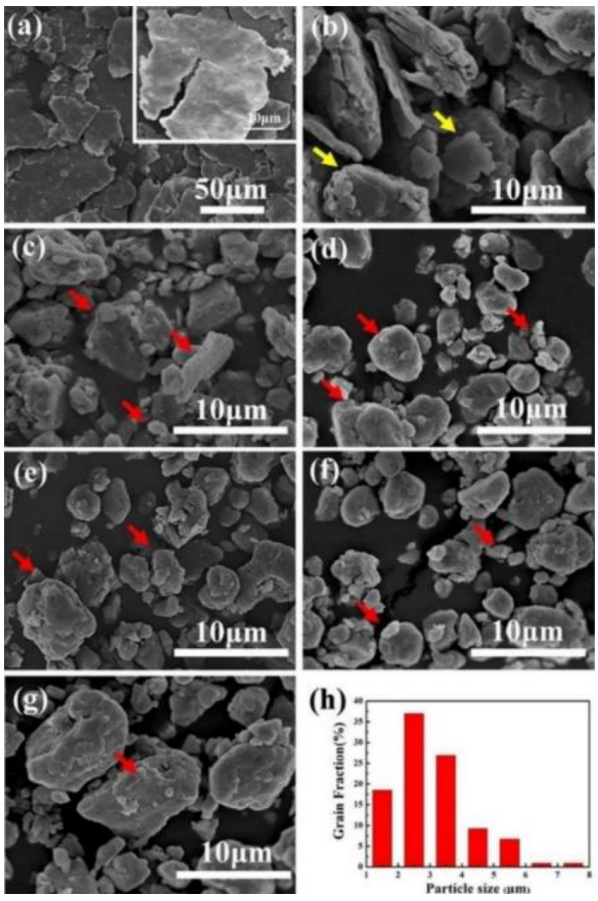


Figure 2: Al-7Zn-2.5Cu-2.5Mg powder morphologies after various ball milling times **(a)** P5, **(b)** P10, **(c)** P15, **(d)** P20, **(e)** P25, **(f)** P30, **(g)** P40, and **(h)** histogram of P30 particles size distribution[18].

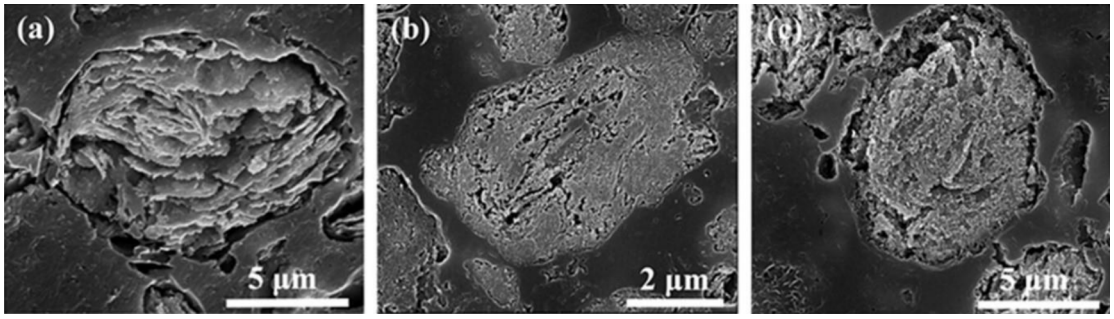


Figure 3: Al-7Zn-2.5Cu-2.5Mg milled powder cross-section morphologies at various ball milling times (P10, P20, and P30)[19].

Table 1: Variation in ball milling times with varied grain sizes and microscopic strain[20].

Sample	Grain Size d (nm)	Micro Strain ε (%)
P5	58.9 ± 3.9	0.053 ± 0.0083
P10	49.1 ± 1.9	0.138 ± 0.0069
P15	51.1 ± 2.4	0.177 ± 0.0076
P20	28.9 ± 0.6	0.135 ± 0.0075
P25	28.0 ± 0.7	0.164 ± 0.0074
P30	22.3 ± 0.6	0.156 ± 0.0072
P40	23.0 ± 0.5	0.138 ± 0.0084

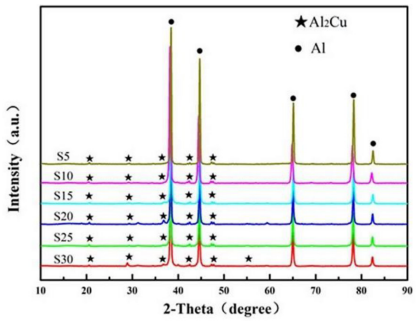


Figure 5: Sintered samples XRD patterns after various ball milling times[22].

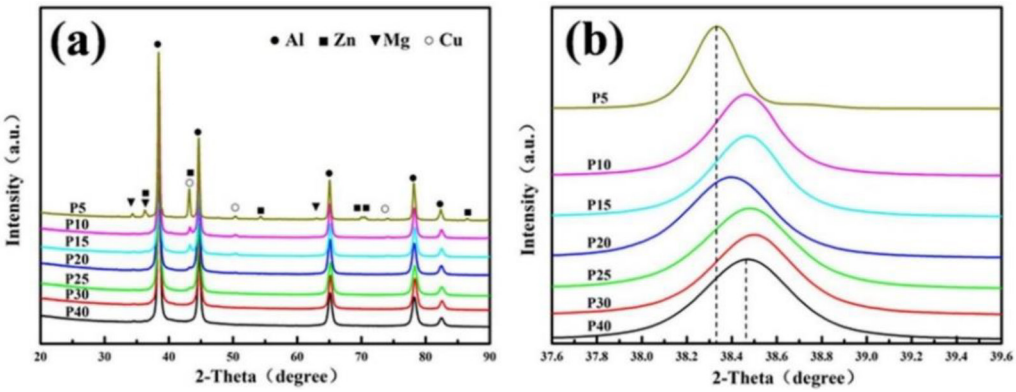


Figure 4: Al-7Zn-2.5Mg-2.5Cu alloy powders X-ray diffraction spectra after various ball milling times, showing **(a)** the overall patterns and **(b)** localized peak patterns[21].

sintered Al-7Zn-2.5Cu-2.5Mg samples. The formation of the intermetallic compound Al_2Cu was observed due to the presence of a supersaturated solid solution of Cu in α-Al, resulting from mechanical alloying. Grain sizes of sintered samples were determined using the Williamson-Hall method, with the smallest grain size measuring 53.5 nm. The microstructure evolved with increasing ball milling time, with the S10 sample exhibiting a lamellar structure, S20 showing a more compact structure, and S30 displaying the most compact structure with smaller and dispersed pores. Longer milling times resulted in finer spherical powders, enhanced sintering, reduced stress concentration, and improved properties, including electrical and thermal conductivity. The shape of ball-milled powders played a crucial role in determining the microstructure, with spherical powders facilitating denser microstructures and enhanced properties. The incorporation of nano

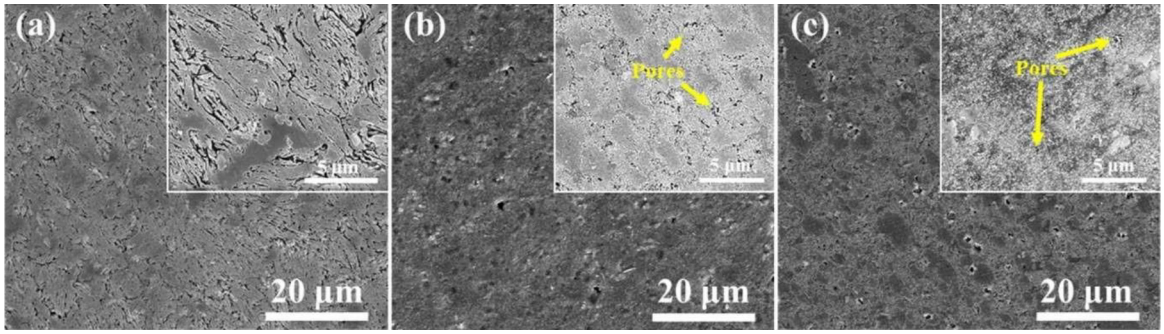


Figure 6: Sintered samples with varying ball milling times are shown in the SEM micrographs in **(a)** S10, **(b)** S20, and **(c)** S30[23].

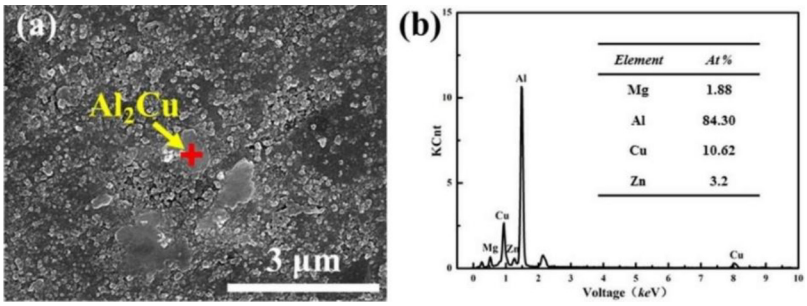


Figure 7: SEM micrograph of the S30 sample microstructure and secondary phase energy-dispersive spectroscopy analysis[24].

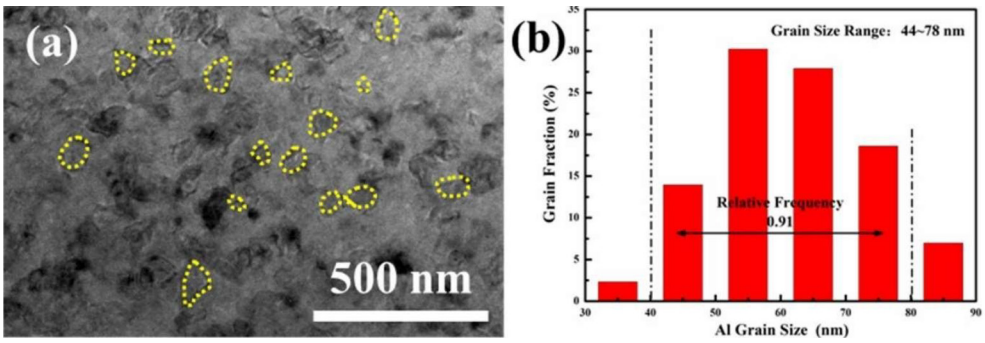


Figure 8: **(a)** A TEM image taken in S30, and **(b)** Distribution histogram of the size of aluminium grains[25].

sized $MgZn_2$ nanoparticles through Spark Plasma Sintering (SPS) led to improved mechanical properties, particularly strength and toughness, by reducing the particle size of the reinforcing phase to less than 50 nanometres. Compressive properties and Vickers microhardness of sintered samples improved with longer milling times, with S30 exhibiting the best comprehensive properties. Fracture surface analysis indicated distinct characteristics, with the S20 sample displaying brittle fracture characteristics with stress concentration points, while the S30 sample exhibited ductile fracture behaviour with enhanced resistance to crack initiation and growth. Overall, the study demonstrated the effectiveness of the SPS process in producing high-strength and hard materials with improved comprehensive properties through controlled milling times and microstructural refinement[33].

4.0 Comparative Analysis

In Case 1, sintered samples exhibited incomplete sintering with a lamellar microstructure characterized by large and irregular α-Al grains. In contrast, Case 2 displayed well-sintered samples with a compact microstructure featuring fine and dispersed α-Al grains. The inclusion of $MgZn_2$ nanoparticles in Case 2 led to the formation

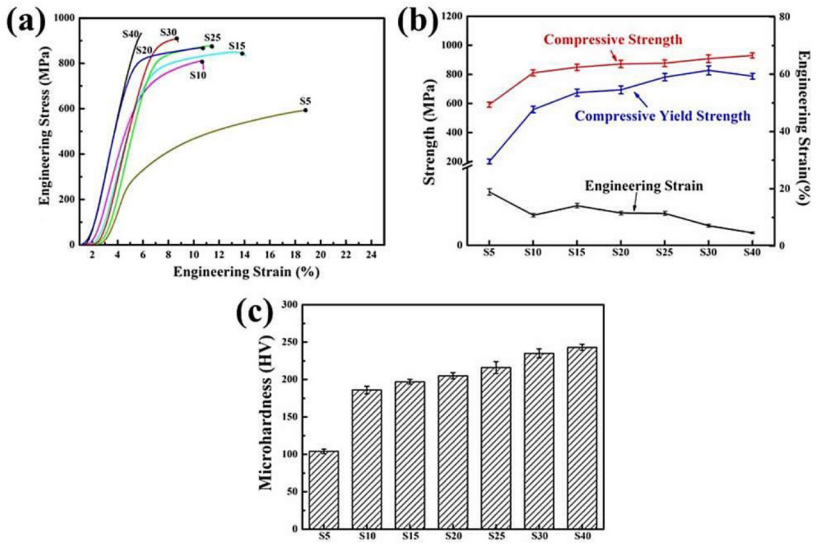


Figure 9: Sintered samples for various ball milling times for the following: **(a)** compressive stress-strain curves; **(b)** strength and strain values; and **(c)** Vickers microhardness[26].

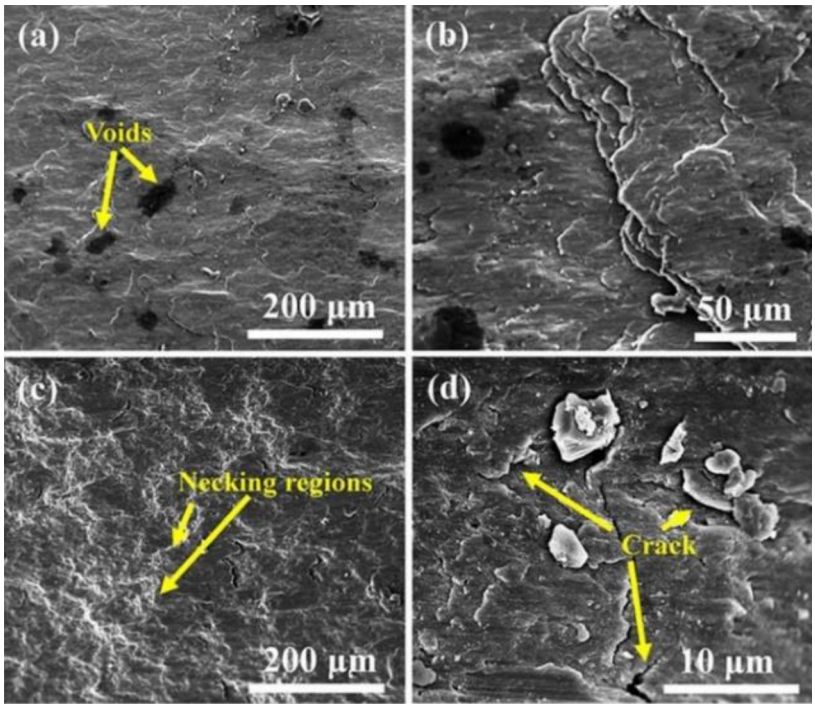


Figure 10: Fracture surface of samples tested under compression: **(a,b)** S20 and **(c,d)** S30[27].

of polygonal-shaped nanoparticles with distinct grain boundaries, further enhancing the microstructure. Regarding mechanical properties, Case 2 outperformed Case 1. It demonstrated superior strength, hardness, and wear resistance. The fine and dispersed α-Al grains in Case 2 minimized grain boundaries and efficiently transferred loads, contributing to increased strength[34]. Additionally, the incorporation of $MgZn_2$ nanoparticles further improved strength and toughness. Moreover, the presence of $MgZn_2$ nanoparticles enhanced the material's wear resistance, making it suitable for applications requiring high durability.

5.0 Discussion

Comparing Case 1 and Case 2 highlights the influence of processing parameters on sintered samples. Case 1, with shorter ball milling and no nanoparticles, yielded lamellar microstructures with incomplete densification and large α-Al grains. In contrast, Case 2, with extended milling and $MgZn_2$ nanoparticles, showed a compact microstructure with fine α-Al grains and polygonal $MgZn_2$ nanoparticles. Mechanically, Case 2 excelled, demonstrating superior strength, hardness, and wear resistance. This underscores the importance of optimizing processing conditions and nanoparticle inclusion for desired microstructures and enhanced mechanical performance in metal matrix composites[35].

6.0 Conclusion

Future research should prioritize comprehensive mechanical characterization, including tensile, compressive, and fatigue testing, to understand material behaviour better. Exploring a wider range of processing parameters like sintering conditions is crucial for uncovering their effects on microstructure and mechanical performance. The use of advanced characterization techniques such as electron microscopy and spectroscopy can provide more detailed analysis. Establishing a strong correlation between material properties and performance metrics for specific applications is essential. Optimizing ball milling parameters like speed and ratio remains crucial for fine-tuning microstructure and properties of sintered materials. This study highlights the importance of ball milling time and calls for further research to advance material processing using these techniques.

7.0 References

1. Shashanka R, Chaira D. Effects of Nano-Y_2O_3 and Sintering Parameters on the Fabrication of PM Duplex and Ferritic Stainless Steels. Acta Metallurgica Sinica. 2016; 29:58-71. Doi: 10.1007/s40195-015-0362-1.
2. Suryanarayana C. Mechanical alloying: a novel technique to synthesize advanced materials. Research. 2019; 2019:1-17. Doi: 10.34133/2019/4219812.
3. Rajendrachari S. An Overview of High-Entropy Alloys Prepared by Mechanical Alloying Followed by the Characterization of Their Microstructure and Various Properties. Alloys. 2022; 1:116-34. Doi: 10.3390/alloys1020008.
4. Shashanka R, Chaira D. Optimization of milling parameters for the synthesis of nano-structured duplex and ferritic stainless-steel powders by high energy planetary milling. Powder Technology. 2015; 278:35-45. Doi: 10.1016/j.powtec.2015.03.007.
5. Shashanka R, Chaira D. Development of nano-structured duplex and ferritic stainless steels by pulverisette planetary milling followed by pressureless sintering. Materials Characterization. 2015; 99:220-229. Doi: 10.1016/j.matchar.2014.11.030.
6. Shashanka R, Chaira D. Phase transformation and microstructure study of nano-structured austenitic and ferritic stainless-steel powders prepared by planetary milling. Powder Technology. 2014; 259:125-36. Doi: 10.1016/j.powtec.2014.03.061.
7. Mahale RS, Shamanth V, Sharath PC, *et al.* Mechanical testing of spark plasma sintered materials: a review. AIP Conf Proc. 2023; 2469:020026-1-020026-24. Doi: 10.1063/5.0080183.
8. Mahale RS, Rajendrachari S, Shamanth V, Krishna H. Technology and challenges in additive manufacturing of duplex stainless steels. Biointerface Research in Applied Chemistry. 2021; 12:1110-9. Doi: 10.33263/briac121.11101119.
9. Mahale RS, Shamanth V, Sharath PC, *et al.* Electrochemical determination of ascorbic acid by mechanically alloyed super duplex stainless steel powders. Metals. 2023; 13(8):1430. Doi: 10.3390/met13081430.
10. Mahale RS, Shamanth V, Sharath PC. Review on processing and characterization of duplex stainless steels. Lecture Notes in Mechanical Engineering. 2020; 219-29. Doi: 10.1007/978-981-15-7557-0_20.
11. Azimi A, Shokuhfar A, Zolriasatein A. Nanostructured Al–Zn–Mg–Cu–Zr alloy prepared by mechanical alloying followed by hot pressing. Materials Science and Engineering: A. 2014; 595:124-130. Doi: 10.1016/j.msea.2013.11.094.
12. Molnarova O, Málek P, Lukac F, Chraska T. Spark plasma sintering of a gas atomized al7075 alloy: microstructure and properties. Materials. 2016; 9:1004. Doi: 10.3390/ma9121004.
13. Becker H, Dopita M, Straska J, Málek P, Vilemova M, Rafaja D. Microstructure and Properties of Spark Plasma Sintered Al-Zn-Mg-Cu Alloy. Acta Physica Polonica A. 2015; 128:602-5. Doi: 10.12693/aphyspola.128.602.
14. Matsuki K, Iwaki T, Tokizawa M, Murakami Y. Microstructural evolution during initial stage of high strain rate superplastic deformation in powder metallurgical 7475 Al–0·7Zr alloy. Materials Science and Technology. 1991; 7:513-9. Doi: 10.1179/mst.1991.7.6.513.
15. Li F, Liu Y, Yi J. Microstructural evolution of gas atomized Al–Zn–Mg–Cu–Zr powders during semi-solid rolling process. Transactions of Nonferrous Metals Society of China. 2014; 24:2475-81. Doi: 10.1016/s1003-6326(14)63373-2.

16. Jeyakumar M, Kumar S, Gupta GS. Microstructure and properties of the spray-formed and extruded 7075 Al Alloy. Materials and Manufacturing Processes. 2010; 25:777-85. Doi: 10.1080/10426910903447253.
17. Rokni MR, Widener CA, Crawford GA. Microstructural evolution of 7075 Al gas atomized powder and high-pressure cold sprayed deposition. Surface and Coatings Technology. 2014; 251:254-63. Doi: 10.1016/j.surfcoat.2014.04.035.
18. Nagae T, Yokota M, Nose M, Tomida S, Otera K, Kamiya T, Saji S. Microstructure and mechanical properties of gas atomized aluminum alloy powder compact densified by pulsed current pressure sintering process. Materials Transactions. 2002; 43:537-43. Doi: 10.2320/matertrans.43.537.
19. Orrù R, Licheri R, Locci AM, Cincotti A, Cao G. Consolidation/synthesis of materials by electric current activated/assisted sintering. Materials Science and Engineering: R: Reports. 2009; 63:127-287. Doi: 10.1016/j.mser.2008.09.003.
20. Fecht H-J. Nanostructure formation by mechanical attrition. Nanostructured Materials. 1995; 6:33-42. Doi: 10.1016/0965-9773(95)00027-5.
21. Turba K, Malek P, Rauch EF, Cieslar M. High Strain Rate Superplasticity in a Zr and Sc Modified 7075 Aluminum Alloy Produced by ECAP. Materials Science Forum. 2008; 584-586:164-9. Doi: 10.4028/www.scientific.net/msf.584-586.164.
22. Malek P, Turba K, Cieslar M, Harcuba P. Microstructure and high temperature deformation of an ultra-fine grained ECAP AA7075 aluminium alloy. International Journal of Materials Research. 2013; 104:3-10. Doi: 10.3139/146.110833.
23. Molnarova O, Malek P, Vesely J, Minarik P, Lukac F, Chraska T, Novak P, Prusa F. The influence of milling and spark plasma sintering on the microstructure and properties of the Al7075 alloy. Materials. 2018; 11:547. Doi: 10.3390/ma11040547.
24. Xia P, Liu Z, Bai S, Lu L, Gao L. Enhanced fatigue crack propagation resistance in a superhigh strength Al–Zn–Mg–Cu alloy by modifying RRA treatment. Materials Characterization. 2016; 118:438-445. Doi: 10.1016/j.matchar.2016.06.023.
25. Ma K, Wen H, Hu T, Topping TD, Isheim D, Seidman DN, Lavernia EJ, Schoenung JM. Mechanical behavior and strengthening mechanisms in ultrafine grain precipitation-strengthened aluminum alloy. Acta Materialia. 2014; 62:141-55. DOI: 10.1016/j.actamat.2013.09.042.
26. Zhao YH, Liao XZ, Jin Z, Valiev RZ, Zhu YT. Microstructures and mechanical properties of ultrafine grained 7075 Al alloy processed by ECAP and their evolutions during annealing. Acta Materialia. 2004; 52:4589-99. Doi: 10.1016/j.actamat.2004.06.017.
27. Huskins EL, Cao B, Ramesh KT. Strengthening mechanisms in an Al–Mg alloy. Materials Science and Engineering: A. 2010; 527:1292-8. Doi: 10.1016/j.msea.2009.11.056.
28. Li H, Wang X, Chai L, Wang H, Chen Z, Xiang Z, Jin T. Microstructure and mechanical properties of an in-situ TiB_2/Al-Zn-Mg-Cu-Zr composite fabricated by Melt-SHS process. Materials Science and Engineering: A. 2018; 720:60-8. Doi: 10.1016/j.msea.2018.02.025.
29. Li CL, Mei QS, Li JY, Chen F, Ma Y, Mei XM. Hall-Petch relations and strengthening of Al-ZnO composites in view of grain size relative to interparticle spacing. Scripta Materialia. 2018; 153:27-30. Doi: 10.1016/j.scriptamat.2018.04.042.
30. Kendig KL, Miracle DB. Strengthening mechanisms of an Al-Mg-Sc-Zr alloy. Acta Materialia. 2002; 50:4165-75. Doi: 10.1016/s1359-6454(02)00258-6.
31. Miller WS, Humphreys FJ. Strengthening mechanisms in particulate metal matrix composites. Scripta Metallurgica et Materialia. 1991; 25:33-38. Doi: 10.1016/0956-716x(91)90349-6.
32. Li B, Sun F, Cai Q, Cheng J, Zhao B. Effect of TiN nanoparticles on microstructure and properties of Al2024-TiN nanocomposite by high energy milling and spark plasma sintering. Journal of Alloys and Compounds. 2017; 726:638-50. Doi: 10.1016/j.jallcom.2017.08.021.
33. Marlaud T, Deschamps A, Bley F, Lefebvre W, Baroux B. Influence of alloy composition and heat treatment on precipitate composition in Al–Zn–Mg–Cu alloys. Acta Materialia. 2010; 58:248-60. Doi: 10.1016/j.actamat.2009.09.003.
34. Queudet H, Lemonnier S, Barraud E, Guyon J, Ghanbaja J, Allain N, Gaffet E. Effect of heat treatments on the microstructure of an ultrafine-grained Al-Zn-Mg alloy produced by powder metallurgy. Materials Science and Engineering: A. 2017; 685:71-8. Doi: 10.1016/j.msea.2016.12.109.
35. Queudet H, Lemonnier S, Barraud E, Guyon J, Ghanbaja J, Allain N, Gaffet E. One-step consolidation and precipitation hardening of an ultrafine-grained Al-Zn-Mg alloy powder by Spark Plasma Sintering. Materials Science and Engineering: A. 2017; 685:227-34. Doi: 10.1016/j.msea.2017.01.009.